

See discussions, stats, and author profiles for this publication at: <https://www.researchgate.net/publication/231668442>

# Measurement of Forces between Spontaneous Vesicle-Forming Bilayers

ARTICLE *in* LANGMUIR · NOVEMBER 1995

Impact Factor: 4.46 · DOI: 10.1021/la00011a016

---

CITATIONS

46

---

READS

8

7 AUTHORS, INCLUDING:



**Shiv Chiruvolu**

NanoGram Corporation

24 PUBLICATIONS 805 CITATIONS

SEE PROFILE



**Zhenghe Xu**

University of Alberta

335 PUBLICATIONS 7,010 CITATIONS

SEE PROFILE

# Measurement of Forces between Spontaneous Vesicle-Forming Bilayers

S. Chiruvolu, J. N. Israelachvili, E. Naranjo, Z. Xu,<sup>†</sup> and J. A. Zasadzinski\*

Department of Chemical Engineering, University of California,  
Santa Barbara, California 93106

E. W. Kaler and K. L. Herrington<sup>‡</sup>

Department of Chemical Engineering, University of Delaware, Newark, Delaware 19716

Received March 31, 1995. In Final Form: July 24, 1995<sup>©</sup>

The forces between bilayers self-assembled onto mica from dilute aqueous solutions containing vesicles of mixed cationic surfactant cetyltrimethylammonium tosylate (CTAT) and anionic surfactant sodium dodecylbenzenesulfonate (SDBS) were measured using the surface forces apparatus. At large separations ( $D > 20$  Å) the forces can be described by the DLVO theory of repulsive electrostatic and attractive van der Waals forces; in dilute solution, the electrostatic repulsion is sufficient to make the net interaction of the mixed surfactant bilayers repulsive at all separations. The electrostatic force dominates any undulation or other long-range interactions and is sufficient to render the vesicles stable against aggregation in dilute solution. Although the net interactions between the mixed surfactant bilayers were monotonically repulsive, fusion of the bilayers could be induced at applied pressures orders of magnitude lower than for single-component phospholipid or surfactant bilayers. At sufficiently high concentrations of added salt ( $> 0.5$  M), the electrostatic interactions were screened sufficiently that multilayers were trapped between the surfaces. The measured forces correlate well with the ternary phase diagram and the vesicle microstructures observed using freeze-fracture and cryo-electron microscopy.

## Introduction

Understanding the magnitude and origin of the forces between bilayer membranes is necessary to understanding the stability of unilamellar vesicles against adhesion and fusion.<sup>1-3</sup> This is especially important for differentiating between metastable mechanically or chemically formed vesicles (whose equilibrium form is often a multilayered lamellar phase)<sup>4-15</sup> and spontaneous or equilibrium vesicles.<sup>16-26</sup> Quite often, colloidal particles can exhibit

remarkable metastability and times to reach true equilibrium can be long.<sup>1</sup> Typical mechanically formed vesicles aggregate and fuse into multilayered liposomes over hours to days.<sup>3-7</sup> To minimize vesicle aggregation, fusion, and eventual failure, standard colloidal stabilization techniques have been used to enhance intervesicle repulsion by steric<sup>9</sup> (appending a bulky polymer-like head group to some fraction of the vesicle lipids) or electrostatic interactions<sup>10</sup> (adding charged surfactants to the bilayers). A second approach to stabilization is the polymerization of the head or tail groups of mechanically formed vesicles.<sup>8,11</sup> Polymerization impedes fusion through the decreased mobility of oligomers as opposed to monomers. However, these methods typically prolong vesicle lifetimes, rather than make the vesicles unconditionally stable.

A better solution is to produce spontaneous equilibrium vesicles by appropriate control of the self-assembly process or by modifying bilayer interactions. There are now quite a variety of "equilibrium" unilamellar vesicles of various chemical compositions discussed in the literature;<sup>16-26</sup> here we are concerned with vesicles prepared from mixtures of anionic and cationic (often referred to as "catanionic")

\* To whom correspondence should be addressed.

<sup>†</sup> Current address: Department of Mining and Metallurgical Engineering, McGill University, Montreal, Canada H3A2A7.

<sup>‡</sup> Current address: W. L. Gore and Associates, 297 Blue Ball Road, Elkton, MD 21921.

© Abstract published in *Advance ACS Abstracts*, October 1, 1995.

(1) Israelachvili, J. N. *Intermolecular and Surface Forces*; Academic Press: London, 1991.

(2) Helm, C. A.; Israelachvili, J. N.; McGuigan, P. M. *Science* **1989**, *246*, 919; *Biochemistry* **1992**, *31*, 1794.

(3) Bailey, S. M.; Chiruvolu, S.; Israelachvili, J. N.; Zasadzinski, J. A. *Langmuir* **1990**, *6*, 1326.

(4) Hui, S. W.; Stewart, T. P.; Boni, L. T.; Yeagle, P. L. *Science* **1981**, *212*, 921.

(5) Verkleij, A. J.; Mombers, C.; Leunissen-Bijvelt, J.; Ververgaert, P. H. *Nature* **1979**, *279*, 162.

(6) Hope, M. J.; Wong, K. F.; Cullis, P. R. *J. Electron. Microsc. Tech.* **1989**, *13*, 277.

(7) Szoka, F., Jr.; Papahadjopoulos, D. *Annu. Rev. Biophys. Bioeng.* **1980**, *9*, 467.

(8) Fendler, J. H. *Membrane Mimetic Chemistry*; Wiley: New York, 1983; Fendler, J. H. *Science* **1984**, *223*, 888.

(9) Lasic, D. *Liposomes: From Physics to Applications*; Elsevier: Amsterdam, 1993.

(10) Hauser, H.; Gains, N.; Eibl, H. J.; Müller, M.; Wehrli, E. *Biochemistry* **1986**, *25*, 2126.

(11) Gros, L.; Ringsdorf, H.; Schupp, H. *Angew. Chem., Int. Ed. Engl.* **1981**, *20*, 305.

(12) Nozaki, Y.; Lasic, D. D.; Tanford, C.; Reynolds, J. A. *Science* **1982**, *217*, 366.

(13) Mayer, L. D.; Hope, M. J.; Cullis, P. R. *Biochim. Biophys. Acta* **1986**, *858*, 161.

(14) Hauser, H.; Mantsch, H. H.; Casal, H. L. *Biochemistry* **1990**, *29*, 2321.

(15) Gamon, B. L.; Virden, J. W.; Berg, J. C. *J. Colloid Interface Sci.* **1989**, *132*, 125.

(16) Hargreaves, W. R.; Deamer, D. W. *Biochemistry* **1978**, *17*, 3759.

(17) Talmon, T.; Evans, D. F.; Ninham, B. W. *Science* **1983**, *221*, 1047; Brady, J. E.; Evans, D. F.; Kachar, B.; Ninham, B. W. *J. Am. Chem. Soc.* **1984**, *106*, 4279.

(18) Kaler, E. W.; Murthy, A. K.; Rodriguez, B. E.; Zasadzinski, J. A. *Science* **1989**, *245*, 1371.

(19) Kaler, E. W.; Herrington, K. L.; Murthy, A. K.; Zasadzinski, J. A. *J. Phys. Chem.* **1992**, *96*, 6698.

(20) Herrington, K. L.; Kaler, E. W.; Miller, D. D.; Zasadzinski, J.; Chiruvolu, S. *J. Phys. Chem.* **1993**, *97*, 13792.

(21) Ambühl, M.; Bangerter, F.; Luisi, P. L.; Skrabal, P.; Watzke, H. *J. Langmuir* **1993**, *9*, 36.

(22) Chiruvolu, S.; Warriner, H.; Naranjo, E.; Idziak, S. H. J.; Radler, J. O.; Plano, R. J.; Zasadzinski, J. A.; Safinya, C. R. *Science* **1994**, *266*, 1222.

(23) Hoffman, H.; Thunig, C.; Munkert, U.; Meyer, H. W.; Richter, W. *Langmuir* **1992**, *8*, 2629.

(24) Porte, G.; Marginan, J.; Basserau, P.; May, R. *Europhys. Lett.* **1988**, *7*, 713.

(25) Coulon, C.; Roux, D.; Bellocq, A.-M. *Phys. Rev. Lett.* **1991**, *66*, 1709.

(26) Herve, P.; Roux, D.; Bellocq, A.-M.; Nallet, F.; Gulik-Krzwicki, T. *J. Phys. II* **1993**, *3*, 1255.

single-tailed surfactants.<sup>18-21</sup> Although dispersing these catanionic surfactants in water is a quite general method for preparing spontaneous equilibrium vesicles,<sup>18-21</sup> the stability of these vesicles against aggregation is not understood. Unlike unilamellar vesicles prepared by mechanical and chemical treatment of multilayered liposomes,<sup>3-15</sup> those formed from catanionic surfactants remain stable and do not aggregate over periods of years. The extent of the vesicle phases in these mixtures shows the vesicles to be stable against aggregation even at volume fractions approaching close packing (about 3% by weight, see Figure 8A).<sup>18-21,27</sup> The lamellar phases in these mixtures also show a single-phase region up to about 80 wt % water, unlike typical phospholipid lamellar phases that are stable only up to about 30–40 wt % water.<sup>22</sup> At intermediate water fractions, a two phase coexistence regime exists between multilamellar liposomes and unilamellar vesicles in the catanionic mixtures, as opposed to primarily dispersions of multilamellar liposomes in excess water for the phospholipid systems. This suggests that the net interaction between the bilayers of catanionic vesicles is inherently more repulsive than that of typical phospholipid bilayers in which a distinct attractive minima exists at a separation of a few nanometers.<sup>1,2</sup> However, the origin of this additional repulsive interaction is not yet fully understood.

A number of phenomenological theories can account for the formation of spontaneously curved vesicles versus planar bilayers at *infinite dilution*, or in the absence of bilayer interactions.<sup>27-32</sup> Nonideal mixing of two surfactant species can lead to a different composition of the monolayers on opposite sides of the bilayer, with corresponding differences in the monolayer spontaneous curvature, and hence to a net spontaneous bilayer curvature.<sup>27</sup> A spontaneous bilayer curvature then renders a vesicle of preferred radius stable in comparison to a flat bilayer. There is good evidence from surface tension,<sup>18-20</sup> conductivity,<sup>19,20</sup> and NMR<sup>21</sup> measurements to show that nonideal mixing does occur in these catanionic systems; physical association between the cationic and anionic surfactants likely produces a long-lived pseudo-double-tailed surfactant. However, such vesicles would be stable against multilayer formation or aggregation only in the limit of a very large bending modulus. When excess anionic or cationic surfactants are present in the bilayer, contributions to the total free energy due to electrostatics of the curved bilayers is more likely to be a stabilizing factor.<sup>29-31</sup> In addition to these theories, thermodynamic models based on molecular packing of single-component and mixed surfactants can also explain vesicle formation in uncharged surfactants both for pure<sup>30,31</sup> and mixed<sup>32</sup> systems; although in these theories, vesicles are stable due to entropic rather than enthalpic reasons and only in very dilute solutions.<sup>27-32</sup>

There are few theoretical or experimental estimates of the nature and magnitude of the interbilayer interactions that differentiate stable catanionic vesicles from unstable phospholipid vesicles at the concentrations observed in our phase diagrams. While a nonzero spontaneous

curvature is useful to help explain a monodisperse population of vesicles, even simple models that compare the bending energy to the energy of an exposed bilayer edge show that closed shells are always preferred to *finite* flat bilayers.<sup>33-35</sup> What is still needed are both experimental and theoretical studies of the interactions between bilayers that lead to spontaneous unilamellar vesicles in catanionic mixtures and multilamellar liposomes in typical double-tailed phospholipids.

The *surface forces apparatus* (SFA) has been used extensively for direct measurement of forces between mica surfaces coated with surfactant or lipid monolayers and bilayers.<sup>1,2,36-40</sup> Cationic and zwitterionic surfactants readily adsorb onto mica from solution to form bilayers, and the measured forces between two such bilayers correlate well with those between large spherical vesicles in the absence of significant undulation forces. (Anionic surfactants typically do not adsorb due to the net negative charge on mica in contact with water.) Repulsive undulation or "Helfrich" forces<sup>41,42</sup> are suppressed by proximity to the mica substrates as the bilayer fluctuations that give rise to these interactions are quenched by the rigid substrate. Such forces are believed to stabilize other spontaneous vesicle systems in which the bilayer bending elasticity is made sufficiently small, typically by adding alcohols or other cosurfactants to lipid or surfactant bilayers.<sup>22-26</sup> It is also possible that small radius vesicles may have different interactions than large radius vesicles. Notwithstanding these limitations, the interaction between bilayer surfaces measured with the SFA has previously been shown to correspond with the measured interactions between freely suspended sub-micrometer vesicles in dilute solution when undulation forces were negligible.<sup>2,3</sup>

Here we used the SFA to investigate the magnitude, range, and origin of the different forces that control vesicle stability in catanionic surfactant mixtures. We find significant differences between the interactions between catanionic bilayers and phospholipid bilayers, most notably the absence of an adhesive minima in the catanionic system due to large electrostatic interactions between the charged bilayer surfaces when an excess of cation is present in the bilayer. This shows that catanionic vesicles are unconditionally stable against aggregation at dilute concentration. At low surfactant and salt concentrations these electrostatic interactions are roughly an order of magnitude larger than repulsions due to bilayer undulations. However, additional measurements show that at high ionic strength (which occurs in the presence of added electrolyte, at the surfactant concentrations present near the transition from the vesicle to the lamellar phase, and in the lamellar phase), screening diminishes the electrostatic interactions to the point that requires a different, and as yet, unknown mechanism of bilayer repulsion. In addition, as the phase diagram shows (Figure 1A), vesicle phases occur up to a nearly 1:1 cation to anion ratio, where

(33) Stratton, C. J.; Zasadzinski, J. A.; Elkins, D. *Anat. Rec.* **1988**, *221*, 503.

(34) Zasadzinski, J. A. *Biophys. J.* **1986**, *49*, 1119. Zasadzinski, J. A.; Scriven, L. E.; Davis, H. T. *Phil. Mag. A* **1985**, *51*, 287.

(35) Fromherz, P. *Chem. Phys. Lett.* **1983**, *94*, 259. Fromherz, P.; Ruppel, D. *FEBS Lett.* **1985**, *179*, 155.

(36) Pashley, R. M.; Israelachvili, J. N. *Colloids Surf.* **1981**, *2*, 169.

(37) Marra, J.; Israelachvili, J. N. *Biochemistry* **1985**, *24*, 4608.

(38) Pashley, R. M.; McGuigan, P. M.; Ninham, B. W.; Evans, D. F. *Science* **1985**, *229*, 1088.

(39) Richetti, P.; Kekicheff, P. *Phys. Rev. Lett.* **1992**, *68*, 1951.

(40) Kekicheff, P.; Richetti, P. *Pure Appl. Chem.* **1992**, *64*, 1603.

(41) Helfrich, W. *Z. Naturforsch. A* **1978**, *33A*, 305. Helfrich, W. *J. Phys. (Paris)* **1985**, *46*, 1263.

(42) Safinya, C. R.; Sirota, E. B.; Roux, D.; Smith, G. S. *Phys. Rev. Lett.* **1989**, *62*, 1134. Roux, D.; Safinya, C. R. *J. Phys. (Paris)* **1988**, *49*, 307.

(27) Safran, S. A.; Pincus, P.; Andelman, D. *Science* **1990**, *248*, 354. Safran, S. A.; Pincus, P.; Andelman, D.; Mackintosh, F. C. *Phys. Rev. A* **1991**, *43*, 1071.

(28) Mackintosh, F. C.; Safran, S. A. In *Materials Research Society Symposium Proceedings*; MRS: Pittsburgh, 1992; Vol. 248, p 11.

(29) Herrington, K. L. Ph. D. Thesis, University of Delaware, unpublished, 1994.

(30) Israelachvili, J. N.; Mitchell, D. J.; Ninham, B. W. *J. Chem. Soc., Faraday Trans. 2* **1976**, *72*, 1525.

(31) Israelachvili, J. N. In *Surfactants in Solution*; Mittal, K. L., Bothorel, P., Eds.; Plenum Publishing Co.: New York, Vol. 4, pp 3–33.

(32) Carnie, S.; Israelachvili, J. N.; Pailthorpe, B. A. *Biochim. Biophys. Acta* **1979**, *554*, 340.

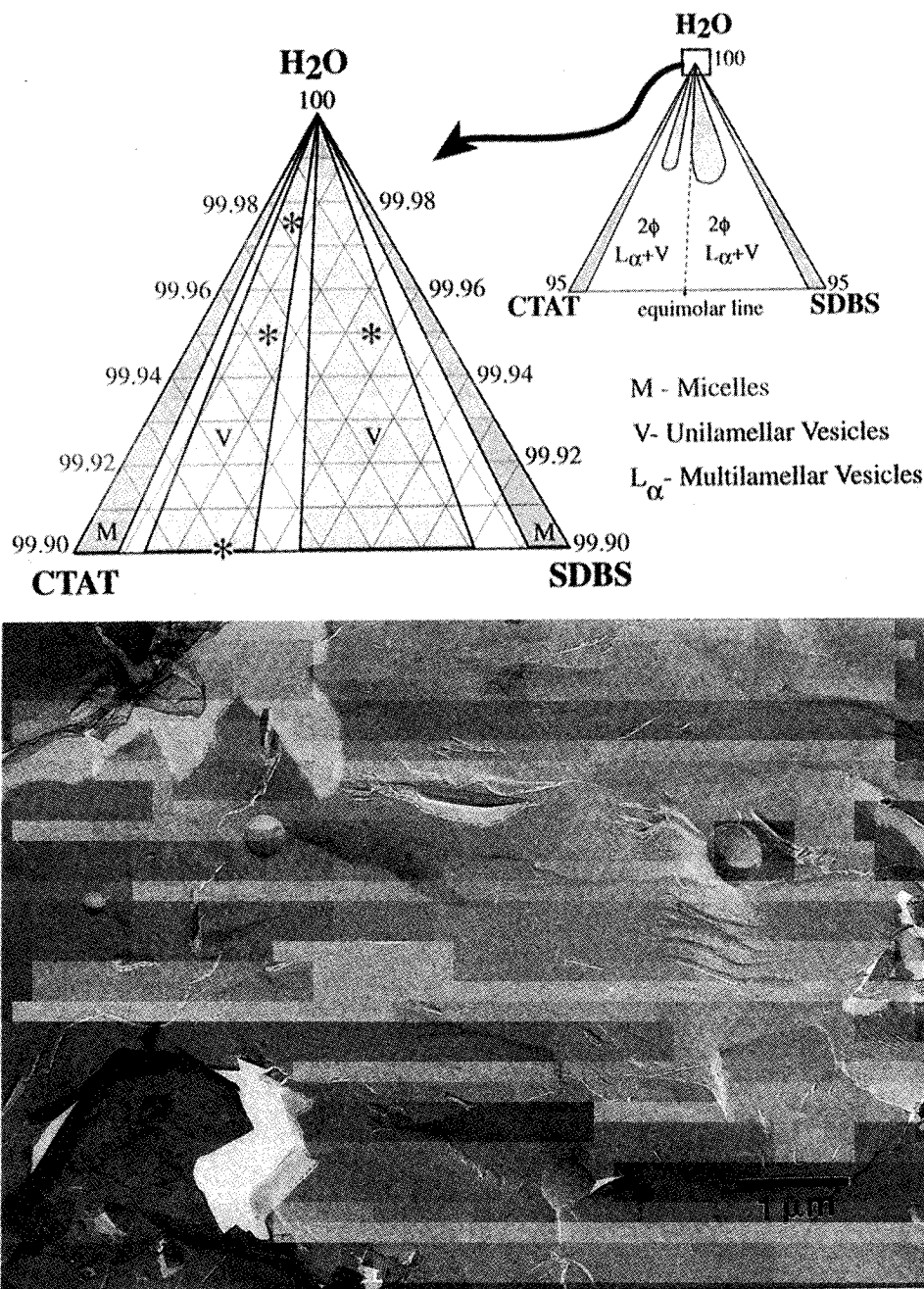


**Figure 1.** (a, top) Ternary phase diagram for CTAT-SDBS-water showing the single phase regions of the vesicles (V) as lobes in the water-rich regions. The asterisks indicate the compositions used in the various experiments. (b, bottom) Freeze-fracture electron micrograph showing a sparse population of typically unilamellar vesicles in a 0.05 wt % CTAT-SDBS (7:3) solution with sizes ranging from 250 Å to 1  $\mu\text{m}$  with an average diameter of 1250 Å.

the bilayers would be nearly neutral and electrostatics should play less of a role. Hence, there is more than one explanation for catanionic vesicle stability over different composition ranges. Future experiments will target the likely candidates for vesicle stabilization such as the Helfrich undulation repulsion (which requires that the catanionic bilayers have a low bending elasticity)<sup>41,42</sup> or the Wennerstrom-Israelachvili steric hydration repulsion (which takes advantage of the relatively high solubility of the single-tailed surfactants in this system).<sup>43</sup>

Although the measured interactions between bilayers were monotonically repulsive, fusion of the bilayers could be induced at applied pressures orders of magnitude lower than for phospholipid bilayers.<sup>2</sup> As bilayer fusion requires nucleation and growth of one or more defects in the bilayer,<sup>2</sup> this reduced pressure for fusion suggests that

the nucleation of such defects is much more facile in catanionic bilayers than in phospholipid bilayers or in single-component surfactants. This may be due to the bilayer edge-stabilizing effect of the excess single-tailed surfactant.<sup>35</sup> In fact, we have observed stable bilayer edges at the surfaces of multilamellar aggregates in the coexistence regime of the phase diagram (see Figure 9B). In general, the measured forces, adhesion and fusion, we measure here correlate extremely well with the ternary phase diagram and the vesicle and other microstructures observed using freeze-fracture and cryo-electron microscopy.<sup>18-20</sup>

### Materials and Methods

Cetyltrimethylammonium tosylate (CTAT) (>99% reported purity), obtained from Alfa Chemicals (Danvers, MA), was recrystallized from a 1:1 mixture of ethanol and acetone. Branched sodium dodecylbenzenesulfonate (SDBS) (99% reported

purity) was used as received from Tokyo Kasei (Japan). Salt (NaCl) which was >99.999% pure was purchased from Aldrich Chemical Co. Measured quantities of crystalline CTAT and SDBS were mixed to the desired weight fractions (70:30 or 30:70) in volumetric flasks, and deionized Milli-Q Plus (Millipore Co., Bedford, MA) water was then added to make up the aqueous dispersions. Solutions were heated briefly to 35 °C and vortexed gently to allow the surfactants to dissolve. To avoid minor variations in composition of the surfactants due to their adsorption on the surfaces of the glassware, the flasks were rinsed at least twice with solutions of the same composition prior to use. Dispersions were then allowed to equilibrate overnight in a water bath at 25 °C prior to use either in the SFA or for sample preparation for electron microscopy. Although this time for equilibration is sufficient for bilayer formation, the time to reach an equilibrium vesicle size distribution can be much longer.<sup>29</sup> However, as we are mainly concerned with the basic bilayer structure confined to a surface, we expect that minor variations in composition that may lead to different vesicle size distributions should not play a major role in the measured interactions as the curvature of the bilayer is set by the mica surfaces. The asterisks on the phase diagram (Figure 1A) mark the concentrations used in these studies, all of which were at CTAT-SDBS ratios of 7:3 or 3:7.

**Cryo-Electron Microscopy.** Samples were prepared in an environmental chamber<sup>44</sup> maintained at >95% humidity at 25 °C. The chamber maintains a constant temperature and near-saturated humidity by circulating the chamber air through a heating element and over sponges saturated with water (or sample liquid). The sample vial was also equilibrated inside the chamber, and thin films of the liquid were formed by first placing a drop of the liquid on a holey carbon TEM grid (Lacey substrates; Ted Pella, Redding, CA) supported on self-locking tweezers. The drop was then blotted with a filter paper to form thin (~1000 Å) films of the liquid sample between the holes of the polymer film. The entire spring-loaded assembly was then vitrified by plunging it into liquid ethane or propane cooled to about 90 K by a surrounding bath of liquid nitrogen. The specimens were transferred from the cryobath under liquid nitrogen and mounted onto a Gatan 626 cold-stage transfer module (Gatan Inc., PA). The sample holder temperature was maintained below -165 °C during imaging using a JEOL 100CX II or a JEOL 2000FX electron microscope operated at 100 kV in the conventional TEM mode. Images were recorded on Kodak SO163 film and processed in undiluted Kodak D-19 developer for 12 min.

**Freeze-Fracture Microscopy.** For FF-TEM, samples were prepared by placing 0.25  $\mu$ L of sample liquid between two thin (0.1 mm) copper freeze-fracture planchettes (Balzers Union BUO-12056-T, Hudson, NH). The sandwiches were allowed to equilibrate in a humidified environmental chamber at 25 °C and > 95% relative humidity.<sup>45</sup> To vitrify the liquid, the sandwich was then plunged into liquid propane cooled by liquid nitrogen. This method of specimen preparation has been shown to give excellent, artifact-free results for aqueous surfactant mixtures.<sup>46</sup> The frozen specimens were then stored under liquid nitrogen until they were transferred to a Balzers 400 freeze etch device. The samples were fractured under vacuum (<10<sup>-7</sup> mbar) at -170 °C and then immediately shadowed with a 20 Å thick layer of platinum deposited at an angle of 45° with respect to the fracture surface, followed by a 100 Å thick layer of carbon deposited normal to the surface. The replicas were allowed to warm up to room temperature, and a second 100 Å layer of carbon was added to increase mechanical strength, making the replicas easier to handle. The samples and replicas were removed from the vacuum chamber, and the samples and copper planchettes were dissolved in chromic acid, leaving the platinum-carbon replicas behind. The replicas were washed in a 50% ethanol-water mixture, rinsed in doubly-distilled water, and collected on formvar-coated 200 mesh gold electron microscope grids (Pelco, Tustin, CA). The replicas were examined using a JEOL 100 CX II transmission electron microscope in the conventional transmission mode using

80 kV accelerating voltage. Images were recorded on Kodak electron-image film.

**Surface Force Apparatus.** The force,  $F$ , between two curved molecularly smooth mica surfaces, shaped as crossed cylinders of radius  $R$ , was measured as a function of separation  $D$  between them using the method and apparatus described by Israelachvili and Adams.<sup>47</sup> The force is measured by a deflection spring method with an accuracy of 10<sup>-7</sup> N, and the separation between the two surfaces was determined optically to an accuracy of  $\pm(1-2)$  Å from the measured fringes of equal chromatic order (FECO) formed from multiple beam interference between the silvered back surfaces of the thin (1-3 mm) mica sheets. The refractive index of the medium between the mica surfaces could also be accurately measured. The shape of the FECO fringes reflects the shape of the curved mica surfaces so that any deformations of the surfaces can be easily observed. Surfactant solutions prepared as mentioned above were directly injected into the SFA chamber, and all force measurements were made after at least 10 min of mixing or equilibration time inside the chamber. In experiments on the effect of total surfactant concentration on the measured forces, a measured volume of the solution was withdrawn from the SFA chamber and was replaced by an equal volume of water. The solution was then thoroughly mixed and allowed to equilibrate overnight before measuring forces at the lowered total surfactant concentration. To change the NaCl salt concentration a known amount of NaCl was added directly to the SFA chamber, thoroughly mixed, and then allowed to equilibrate for at least 30 min prior to resuming the force measurements.

**Analysis of Force Data.** Forces were plotted as log  $F/R$  against  $D$ . Using the Derjaguin approximation,<sup>48</sup> this is equivalent to the corresponding energy per unit area between two flat surfaces. Each experiment was repeated, and the data points were combined for presentation and analysis to avoid systematic errors. To evaluate the force data, theoretically calculated curves were fitted to the experimental data points plotted on a semilogarithmic plot. At large separations, (>25 nm) the log of the interaction forces was linear with separation; a Debye length (and hence the ionic strength of the solution) for each experiment was evaluated from the slope. Theoretical force curves were obtained by summing the nonretarded van der Waals attractive force and the electrostatic repulsive force (obtained by an exact numerical solution of the Poisson-Boltzmann equation for two identical surfaces) and fitting to the data. The former gives the Hamaker constant,  $A$ , for the interaction, and the latter gives the charge density  $\sigma_0$ . The concave upward shape of the force curves at separations less than a Debye length was consistent with surfaces interacting at constant surface charge density.<sup>1</sup> The force curves were insensitive to the value chosen for  $A$ , so all fits were performed with a Hamaker constant of  $7 \times 10^{-21}$  J,<sup>37</sup> reducing the fit to a single parameter,  $\sigma_0$ . The corresponding surface potential  $\psi_0$  was calculated from the fit values of the surface charge density and the Debye length.<sup>1</sup> Theoretically fitted curves are shown by solid lines, and the values of  $\sigma_0$  and  $\psi_0$  are given in the corresponding figure legend.

## Results

**CTAT-Rich Bilayers: Effect of Total Surfactant Concentration.** Figure 1A shows the water-rich corner of the ternary phase diagram for the CTAT-SDBS surfactant-water system.<sup>18-20</sup> The asterisks in Figure 1A mark the concentrations used in the SFA studies, all of which were at CTAT-SDBS ratios of 7:3 or 3:7. These ratios correspond to the greatest extent of the vesicle lobes in the phase diagram. Solutions at these concentrations contain spherical unilamellar vesicles with diameters ranging from about 0.05-0.5  $\mu$ m as shown by freeze-fracture images such as in Figure 1B. The actual concentrations of monomer CTAT and SDBS in these solutions and the weight fraction of CTAT and SDBS in the vesicles can be estimated using a pseudo-phase

(44) Bellare, J. R.; Davis, H. T.; Scriven, L. E.; Talmon, Y. *J. Electron Microsc. Tech.* **1988**, *10*, 87.

(45) Bailey, S.; Chiruvolu, S.; Longo, M.; Zasadzinski, J. J. *J. Electron Microsc. Tech.* **1991**, *19*, 118.

(46) Zasadzinski, J. A.; Bailey, S. M. *J. Electron Microsc. Tech.* **1987**, *91*, 4219.

(47) Israelachvili, J. N.; Adams, G. E. *J. Chem. Soc., Faraday Trans. 1* **1978**, *74*, 975.

(48) Derjaguin, B. V. *Kolloid-Z.* **1934**, *69*, 155.

Table 1

wt % surf	[surf]/ mM	[CTAT] <sub>mon</sub> / mM	[SDBS] <sub>mon</sub> / mM	$Y_{\text{mon}}^a$	$X_{\text{mon}}^b$
0.10	2.4	0.0082	$7.1 \times 10^{-5}$	0.9914	0.6403
0.05	1.2	0.0080	$7.4 \times 10^{-5}$	0.9909	0.6380
0.025	0.6	0.0077	$7.9 \times 10^{-5}$	0.9898	0.6360

<sup>a</sup>  $Y_{\text{mon}}$  is the mole fraction of CTAT in the monomer mix (=mol CTAT<sub>mon</sub>/total monomer). <sup>b</sup>  $X_{\text{mon}}$  is the mole fraction of CTAT in the aggregate. The mole fraction of CTAT in the bulk is 0.6409.

separation model combined with activity coefficients calculated using regular solution theory.<sup>19,20,29</sup> An interaction parameter of  $-23.8$  was calculated following the standard methodology,<sup>29,49</sup> by using the experimental values of surface tension as a function of surfactant concentration for five mixing ratios of CTAT–SDBS ranging from 9:1 to 1:9 by weight. The calculated monomer concentrations are shown in Table 1. For a mixing ratio of 7:3 CTAT–SDBS, the critical aggregation concentration (cac) is  $2.4 \times 10^{-6}$  M, which is roughly 100 times below the critical micelle concentration (cmc) of CTAT (0.24 mM), which is in turn an order of magnitude lower than the most dilute concentration used in these experiments. In this range of concentrations, the calculations show that virtually all of the SDBS is incorporated into the vesicles, which have a composition close to the bulk mixing ratio. The monomer concentration is almost entirely excess CTAT at levels between the cac and the cmc. As it is impossible to measure the local surfactant concentration on the mica surface, we assume throughout that the outer surface of the bilayer adsorbed onto mica has a composition similar to that of the vesicles in solution. For the purposes of these experiments, however, it is not necessary that the actual composition ratio of CTAT to SDBS of the adsorbed bilayer be exactly that of the bulk solution as catanionic vesicles are stable over a wide range of CTAT to SDBS ratios (Figure 1).

Due to the net negative charge of the mica surface in aqueous solution (the result of dissociation of potassium ions from the mica surface<sup>1</sup>), the inner monolayer in contact with the mica surface is most likely enriched in CTAT in order to compensate for the negative charge on the mica. However, numerous SFA experiments have shown that the long-range interactions are dominated by the bilayer surface in contact with the solution; hence the measured interactions should be representative of the intervesicle interactions.<sup>1,2,3, 37</sup> The measured values of surface charge and potential and their variation with surfactant concentration and added salt are consistent with this assumption. The composition asymmetry of the bilayer adsorbed onto mica is also not important to the interactions between bilayers in the SFA (although it would be important in vesicles as it could generate a spontaneous bilayer curvature<sup>27, 28</sup>) as the curvature of the bilayer is fixed by the curvature of the mica surfaces.<sup>27,28</sup>

Figure 2 shows the measured force profiles of bilayers adsorbed from 7:3 CTAT–SDBS vesicle solutions at 0.1, 0.05, and 0.025 wt % total surfactant. At large separations, the linearity of the semilog plot of  $F/R$  versus distance shows that the long-range interactions are electrostatic<sup>1</sup> and increase in range with increasing surfactant dilution from 0.10 to 0.025 wt %, consistent with a screened double-layer interaction. Bilayer–bilayer contact, as determined

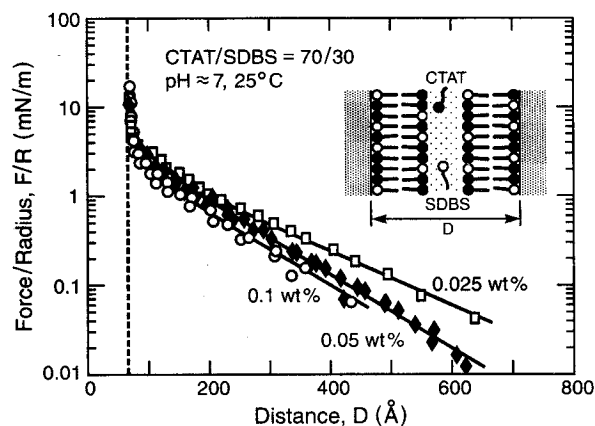


**Figure 2.** Measured forces between mica surfaces in 0.10, 0.05, and 0.025 wt % CTAT–SDBS (7:3) surfactant solutions at pH  $\approx 7$  and  $T = 25^\circ\text{C}$  without added electrolyte. Forces were first measured in a 0.10 wt % solution, added directly to the SFA chamber. The surfactant solution was subsequently diluted and allowed to reequilibrate at 0.05 and 0.025 wt %. The solid lines are the theoretical force curves fitted at constant  $\sigma$  with the following parameters: (i) 0.10 wt %,  $\sigma_o = 6 \text{ mC/m}^2$  and  $\psi_o = 58 \text{ mV}$ ; (ii) 0.05 wt %,  $\sigma_o = 7 \text{ mC/m}^2$  and  $\psi_o = 76 \text{ mV}$ ; and (iii) 0.025 wt %,  $\sigma_o = 6 \text{ mC/m}^2$  and  $\psi_o = 82 \text{ mV}$ . The distance  $D = 0$  is the separation between the mica surfaces before addition of surfactant to the chamber. The dashed vertical line at  $D \approx 63 \text{ \AA}$  corresponds to the “contact” of two adsorbed bilayers each  $31.5 \text{ \AA}$  thick.

from the flattening of the FECO fringes,<sup>35</sup> occurs at  $D \approx 63 \text{ \AA}$ , indicating that each bilayer is  $32 \pm 1 \text{ \AA}$  thick. For 0.10, 0.05, and 0.025 wt % surfactant concentrations, the decay lengths obtained by fitting simple exponential functions to the long-range repulsion were 107, 109, and  $143 \text{ \AA}$ , respectively. For the cation-rich bilayers adsorbed on the surface, these values are systematically larger than the smallest possible theoretical Debye lengths of 62, 88, and  $124 \text{ \AA}$ , respectively, expected if all the ions (tosylate, dodecylbenzene sulfonate ions, sodium, and cetyltrimethylammonium ions) were present in solution. The larger measured than theoretical screening lengths indicate that not all of the ions are “free,” which is due to two factors: (1) partial ionization of the CTAT molecules in the bilayers and (2) the presence of surfactant aggregates in solution.<sup>1,50</sup> The concave upward shapes of the force curves at separations less than a Debye length suggest that the adsorbed bilayers are interacting at constant surface charge density and that the surfactant behaves as a 1:1 electrolyte; a constant surface charge model provided the best fit to the data, and results are shown in the figures. For the three surfactant concentrations, the surface charge density of the adsorbed bilayers,  $\sigma_o \approx 6\text{--}7 \text{ mC/m}^2$ , does not vary significantly, whereas with decreasing surfactant concentration the surface potential increases from  $\psi_o \approx 58$  to  $82 \text{ mV}$ . The value of the surface charge density ( $6\text{--}7 \text{ mC/m}^2$ ) corresponds to one unit charge per  $2500 \text{ \AA}^2$ .

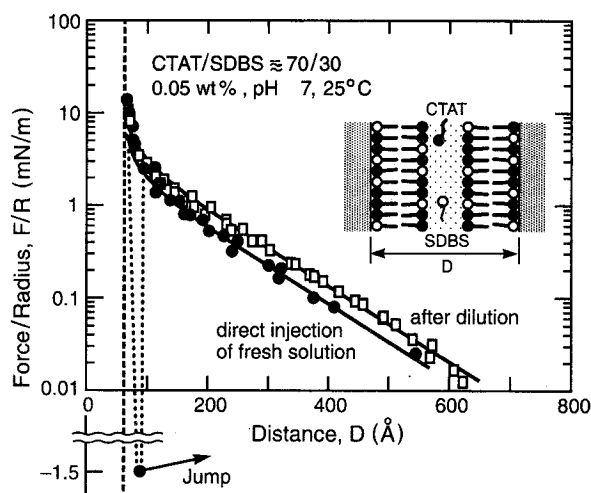
#### CTAT-Rich Bilayers: Direct Injection vs Dilution.

Figure 3 shows a comparison between force profiles for a CTAT–SDBS (7:3) vesicle solution added directly to the SFA at 0.05 wt % and for a solution initially at 0.10 wt %, but subsequently diluted to 0.05 wt %. The repulsive electrostatic force in the directly injected 0.05 wt % solution is slightly weaker than for a system diluted to 0.05 wt %. However, the exponential decay length is in close agreement. For bilayers formed in the freshly injected solution  $\sigma_o$  and  $\psi_o$  were lower, at  $4.5 \text{ mC/m}^2$  and  $57 \text{ mV}$  compared to  $7 \text{ mC/m}^2$  and  $76 \text{ mV}$  for the diluted solution.<sup>50</sup> In addition to the weaker electrostatic repulsive force

(49) Kaler, E. W.; Herrington, K. L.; Miller, D. D.; Zasadzinski, J. A. *In Structure and Dynamics of Supramolecular Aggregates and Strongly Interacting Colloids*; Chen, S. H., Huang, J. S., Tartaglia, P., Eds.; Kluwer Publications: Holland, 1992. Rosen, M. J. *Surfactants and Interfacial Phenomena*, 2nd ed.; Wiley and Sons: New York, 1989.

(50) Kékicheff, P.; Ninham, B. W. *Europhys. Letters* **1990**, *12*, 471.





**Figure 3.** Measured forces between mica surfaces in 0.05 wt % CTAT–SDBS (7:3) surfactant solution added directly to the SFA chamber ( $\sigma_o = 4.5 \text{ mC/m}^2$  and  $\psi_o = 57 \text{ mV}$ ) and after dilution to 0.05 wt % from an initial concentration of 0.10 wt % ( $\sigma_o = 7 \text{ mC/m}^2$  and  $\psi_o = 76 \text{ mV}$ ).

observed in the directly injected solution, a small adhesive force minimum was also observed. In this solution, after initially bringing the surfaces to contact at  $D \approx 63 \text{ Å}$ , on moving them apart the surfaces first become pointed (as seen with the FECO fringes) and then jump apart at  $D = 90 \text{ Å}$  (i.e., from a bilayer–bilayer separation of  $\sim 27 \text{ Å}$ ) with an adhesion force of  $F/R = -1.5 \text{ mN/m}$ . This force curve is quite unlike the purely repulsive force measured with the diluted solution. The difference in forces between the two bilayers adsorbed at different surfactant concentrations can be attributed to minor differences in bilayer structure and composition, likely due to insufficient time for equilibrating the directly injected solution. Adsorption at lower total surfactant concentrations can result in a loosely packed bilayer with lower charges per unit area.<sup>39</sup>

The pointedness of the FECO fringes just prior to the surfaces jumping apart after adhesion means that the two surfaces bend sharply away from each other just outside the contact region. This phenomenon does not seem to have been previously reported, and it is not expected from theories of contact mechanics such as the JKR<sup>51</sup> and DMT<sup>52</sup> theories. However, unlike the more common cases so far studied where the interaction potential is purely attractive at all separations and gives rise to the typical JKR-type flattening deformation illustrated in Figure 4A, the force profile of Figure 3 is highly variable over a short distance regime, going from attraction at “contact” to an extensive repulsive regime at slightly larger separations ( $D > 80\text{--}100 \text{ Å}$ ) before falling to zero at larger separations. This type of interaction potential, which also arises between other types of surfaces whenever a short-ranged attraction (adhesion) is immediately followed by a strong repulsion, causes a sharper deformation of the surfaces at the bifurcation boundary, resulting in the surfaces becoming “pointed” before they separate at an area significantly less than predicted by the JKR equation, as illustrated in Figure 4B. This effect also produces a sharper (more rapid) jump apart on separation because once the surfaces have separated beyond the force barrier, they are helped along by the repulsive force. We are not aware of any previous experimental mention or theoretical treatment of this

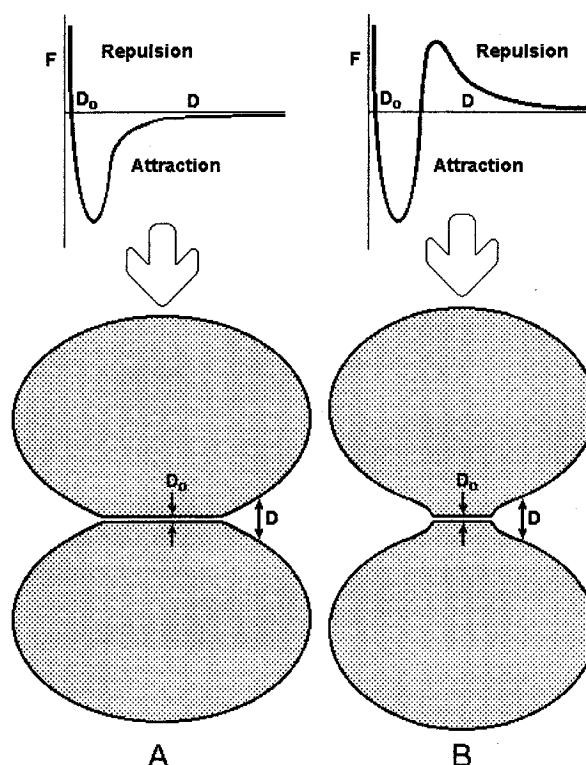


**Figure 4.** Interaction force between two curved elastic surfaces and the different deformations they produce when the surfaces are in adhesive contact at  $D = D_0$ . (A) Purely attractive interaction: JKR type deformation, illustrated for two adhering vesicles. (B) Attractive adhesion regime followed by repulsive regime (cf. Figure 3): surfaces bend away sharply just outside the contact zone to avoid the repulsive force regime. The sharp contact zone appears as a sharp point of the FECO fringes in the SFA.

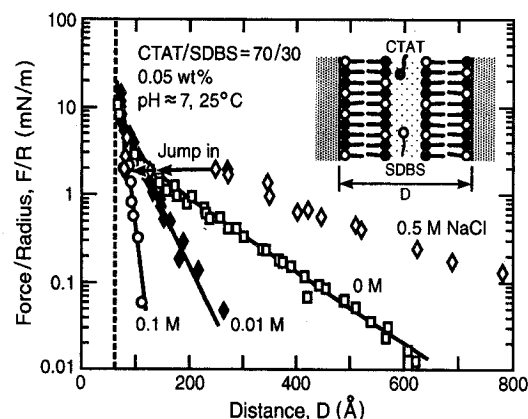


**Figure 5.** Forces between mica surfaces in a 0.05 wt % CTAT–SDBS (7:3) surfactant solution in (i) pure water, 0 M,  $\sigma_o = 7 \text{ mC/m}^2$  and  $\psi_o = 76 \text{ mV}$ ; (ii) 0.01 M NaCl,  $\sigma_o = 18 \text{ mC/m}^2$  and  $\psi_o = 68 \text{ mV}$ ; (iii) 0.10 M NaCl,  $\sigma_o = 28 \text{ mC/m}^2$  and  $\psi_o = 36 \text{ mV}$ ; and (iv) 0.50 M NaCl. The double-layer forces thus varied between constant charge and constant potential.

phenomenon, but it is interesting to note that the existence of a repulsive regime beyond the adhesive minimum appears to affect both the shape and the area of the surfaces at separation, as well as the kinetics of the separation process.

**CTAT-Rich Bilayers: Effect of Electrolyte Concentration/Ionic Strength.** The nature of the repulsive electrostatic forces was also studied as a function of increasing ionic strength for a fixed surfactant concentration of 0.05 wt % (Figure 5). A decreasing range of the repulsion was measured with increasing salt (NaCl) concentration as expected.<sup>1</sup> However, in 0.5 M NaCl

(51) Johnson, K. L.; Kendall, K.; Roberts, A. D. *Proc. R. Soc. London, Ser. A* **1971**, *324*, 301.

(52) Derjaguin, B. V.; Muller, V. M.; Toporov, Y. P. *J. Colloid Interface Sci.* **1975**, *53*, 314.

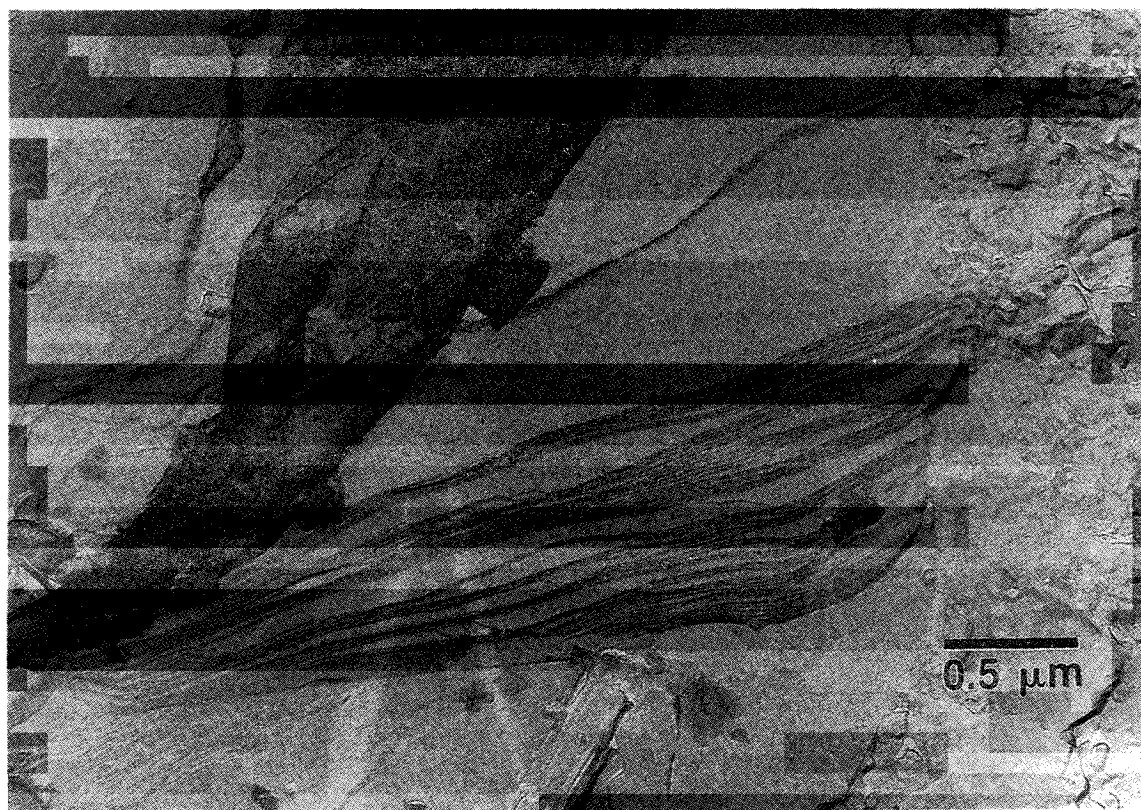


**Figure 6.** Freeze-fracture electron micrograph showing the presence of large multibilayer aggregates adsorbed to the copper planchettes in a 0.05 wt % CTAT-SDBS (7:3) surfactant solution when the salt concentration was increased to 0.50 M.

solution a number of new features appeared. Macroscopically, the vesicle solution loses its foaming ability and becomes more viscous, and a floating "precipitate," resembling the lamellar phase found at higher concentrations, appears. Microscopically, the range of the repulsive interactions appears to increase rather than decrease, although  $F/R$  no longer has a simple exponential decay with distance. Consistent with the macroscopic observations, the movement of the surfaces during force measurements is noticeably more sluggish; erratic drifts set in, and the whole system appears to be mechanically less stable. In addition to the long-range repulsion, there is an instability jump-in from  $\sim 250$  to  $\sim 127$  Å, followed by a spontaneous, but slow, drift-in to 84 Å, at which point the force becomes steeply repulsive. These long-range interactions are somewhat surprising at first as the theoretical value of the screening length at 0.5 M electrolyte is only 4.2 Å.

We believe that by increasing the ionic strength of the solution to 0.5 M, the electrostatic repulsion is screened sufficiently to allow vesicles in solution to adhere to the adsorbed bilayers where they likely collapse into a lamellar phase (through osmotic stress). The measured jump-in to 127 Å, corresponding to twice the thickness of two bilayers, suggests that this effect occurs during rapid compressions. The subsequent slow approach to  $D \approx 84$  Å indicates that these secondary bilayers also spread out and fuse or incorporate into the primary bilayer on each surface. A freeze-fracture electron micrograph of the 0.5 M NaCl dispersion is shown in Figure 6. The large multilamellar structures in solution are composed of stacked bilayers generated via such adhesions and subsequent fusions, and the vesicles appear to be unstable with respect to a bulk lamellar phase. It is the interactions between these multilamellar stacks adsorbed onto each mica surface that give rise to the measured long-range interactions.

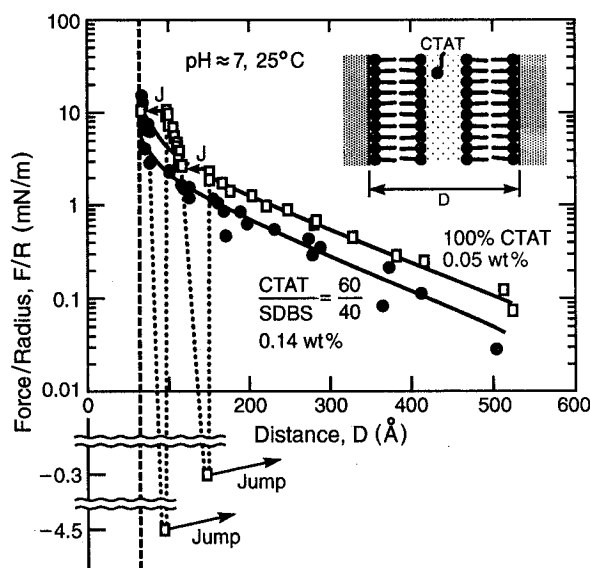


**Figure 7.** Force profiles for pure CTAT at 0.05 wt % ( $\sigma_o = 10$  mC/m<sup>2</sup> and  $\psi_o = 99$  mV) showing two adhesive minima superimposed on an exponentially repulsive force, and the effect of adding SDBS to the solution to a total concentration of about 0.14 wt % at a CTAT-SDBS ratio of 60–40 ( $\sigma_o = 5$  mC/m<sup>2</sup> and  $\psi_o = 64$  mV). Inward jumps are indicated by arrows labeled J.

#### CTAT-Rich Bilayers: Effect of CTAT-SDBS Ratio.

To confirm that the outer monolayer surfaces were representative of the bulk surfactant ratio, we also measured forces in a pure CTAT solution at 0.05 wt %. As seen in Figure 7, for pure CTAT solution at separations greater than 150 Å, an exponentially repulsive double-layer interaction with a screening length of 124 Å was measured (the theoretical minimum value for fully ionized 1:1 electrolytes in solution is 92 Å). At 150 Å a small jump-in occurs to a separation of 112 Å. Further compression resulted in a second jump-in from 94 Å to



final bilayer-bilayer contact at  $D \approx 64$  Å. The period of these jumps or oscillations is about 32 Å, about twice the molecular length of CTAT. The surface charge density of the adsorbed pure CTAT bilayers,  $\sigma_o$ , was 10 mC/m<sup>2</sup>, and the surface potential was  $\psi_o \approx 99$  mV. The outer and inner adhesive minima on the force profile could be measured repeatedly and were found to be  $F/R = -0.30$  and  $-4.5$  mN/m respectively.

On completing the measurements with the pure CTAT solution, part of the solution was extracted and replaced by a concentrated mixed surfactant solution to obtain a final composition of about 0.14 wt % surfactant and a final CTAT-SDBS ratio of 6:4. The new mixture was allowed to equilibrate for  $\sim 45$  min before resuming force measurements. As shown in Figure 7, even with these relatively short equilibration times, addition of SDBS to the surfactant solution eliminates the two adhesive minima and makes the force profile entirely repulsive, as noted earlier for mixed CTAT-SDBS solutions at similar concentrations. The surface charge density,  $\sigma_o \approx 5$  mC/m<sup>2</sup>, and surface potential,  $\psi_o \approx 64$  mV were consistent with our previous measurements of bilayers directly absorbed from the vesicle solutions.

**Fusion of Adsorbed Bilayers.** In addition to measuring interbilayer forces, we also studied pressure-induced fusion of CTAT-rich bilayers. Fusion of mixed bilayers (CTAT-SDBS = 7:3) was first studied in a 0.13 wt % surfactant solution which had been diluted in two steps from 0.50 wt %. Gradual compression of the surfaces beyond bilayer-bilayer contact ( $D \approx 63$  Å) to about 58 Å resulted in fusion which occurred over a period of a few seconds and could be reproduced repeatedly. Subsequent to fusion, the final distance between the mica surfaces was 19 Å, a thickness corresponding to an interdigitated layer of adsorbed surfactant between the two mica surfaces one monolayer thick. The applied pressure to initiate fusion, calculated from the force and flattened contact area at fusion, was  $6 \times 10^4$  Pa or about 0.6 atm. For double-tailed phospholipid bilayers, no fusion was observed even at pressures of 40 atm.<sup>2</sup> Owing to the significant deformation of the surfaces at such high external loads, a quantitative description of the force behavior from 70 to 58 Å was not attempted. However, on separating the fused bilayers, a negligible adhesion energy was measured.

In separate experiments with added salt, the fusion pressure decreased slightly, dropping from  $6 \times 10^4$  Pa in zero M salt to  $4.4 \times 10^4$  Pa in 0.1 M NaCl, then to  $3.3 \times 10^4$  Pa in 0.5 M NaCl. But the corresponding final surface separations remained essentially unchanged at 19, 21, and 25 Å, respectively. In contrast, to induce fusion of bilayers having a higher fraction of SDBS (CTAT-SDBS = 6:4) but at roughly the same total concentration of 0.14 wt %, a significantly higher pressure of  $8.4 \times 10^6$  Pa was needed.

**SDBS-Rich Bilayers.** Forces between mica surfaces were also measured in SDBS-rich (CTAT-SDBS = 3:7) vesicle solutions at 0.05 wt % total surfactant concentration (Figure 8). Although the forces measured in this solution feature a long-range electrostatic repulsion with a screening length of 76 Å, this repulsion continued down to a separation of about 5 Å before a steep increase in the repulsion was noted. From these results it is evident that no bilayers adsorbed on the mica and that the interactions measured are due to the mica surfaces alone. The reason for this lack of adsorption is that SDBS-rich bilayers are negatively charged and are therefore repelled from the negatively charged mica surfaces. All of the CTAT is incorporated into the bilayers at these concentrations,

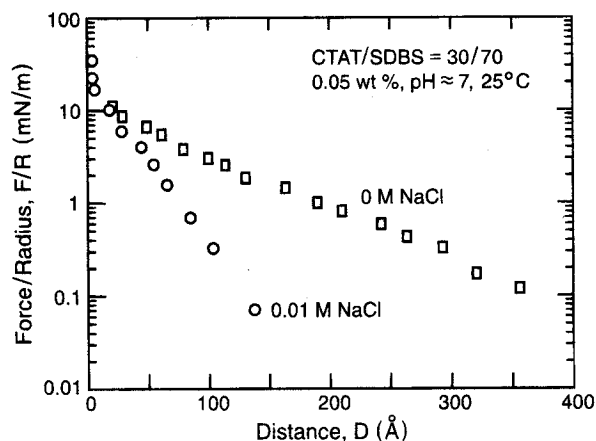


**Figure 8.** Measured forces in 0.05 wt % CTAT-SDBS (3:7) surfactant solution showing repulsive double-layer forces between the mica surfaces with no contribution from any adsorbed bilayer. This indicates that there was negligible adsorption of the negatively charged SDBS-rich bilayers on the negatively charged mica surfaces.

hence there is an insufficient number of free CTA<sup>+</sup> ions to neutralize the negatively charged mica surfaces.

### Discussion

The measured long-range forces between catanionic vesicles in dilute solution are well described by simple double-layer electrostatic repulsion. In CTAT-rich vesicle solutions, at low salt levels, the forces are repulsive at all separations and are well described by the DLVO theory down to bilayer separations of 20 Å. At these separations, an additional repulsion above and beyond the DLVO forces also keeps the bilayers from adhering, although our measurements are not sufficiently accurate to describe the functional form of the interaction or its origin. This agrees well with the solution behavior of the vesicles which remains stable at concentrations virtually up to close packing (see Figure 9A). As discussed below, the addition of electrolyte screens the repulsive interaction between vesicles, and only when 0.5 M salt is added do the vesicles aggregate and fuse and finally form multilamellar structures. The repulsive interactions shown in Figure 2 are roughly an order of magnitude greater than one would expect from undulations, even with a bending modulus as small as  $k_B T$ .<sup>41,42</sup> Hence, the major contribution to the bilayer repulsion and stability against aggregation in catanionic vesicles at low concentration is simply the electrostatic double layer forces generated by the charged membranes.

The measured bilayer thickness of 31–32 Å in CTAT-rich solutions is in close agreement with 33 Å estimated for CTAB.<sup>36</sup> The small difference might be due to the presence of the short-chained component SDBS in the bilayers adsorbed in our experiments. It has been shown earlier that addition of short-tailed cosurfactants thins the bilayer membrane.<sup>42</sup> Our measurements of slightly thinner adsorbed bilayers from CTAT-SDBS vesicle solutions suggests the adsorption of mixed bilayers similar in composition to the vesicles themselves. This observation is confirmed by the lack of adsorption from the SDBS-rich vesicle solution due to mutual repulsion between the negatively charged bilayers and the negatively charged mica surfaces.

We measured a roughly constant surface charge density for three different total surfactant concentrations, i.e., 0.1, 0.05, and 0.025 wt % in the dilution series, which suggests that the composition of the adsorbed bilayers remains approximately the same and that there is a

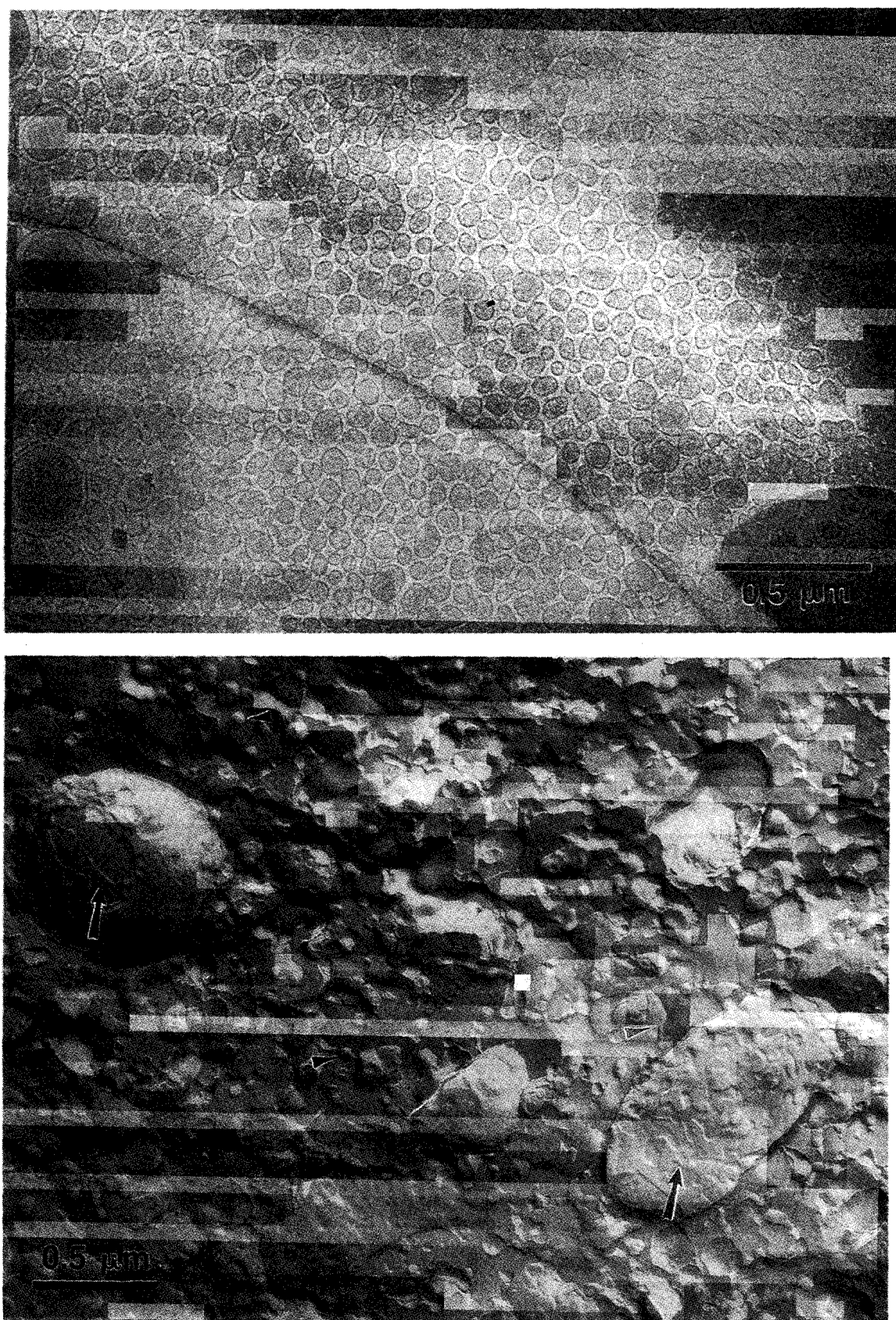


**Figure 9.** (A, top) Cryo-electron micrograph showing close-packed unilamellar vesicles and some multilamellar particles in the vesicle-rich phase of a two-phase sample of 10 total wt % CTAT-SDBS (3:7). (The actual surfactant concentration in the vesicle phase is about 3–4 wt %.) Note the absence of visible adhesion even at this concentration, at which the vesicles are nearly touching. (B, bottom) Multilamellar liposome-rich phase of a 3:2 CTAT-SDBS two-phase sample of total surfactant concentration 9 wt %. The multilamellar aggregate surfaces are highly irregular and convoluted, suggesting stable bilayer edges and unconnected patches of bilayers in contact with water.

negligible amount of monomer surfactant. This is consistent with our calculations of the monomer concentration and vesicle composition presented in Table 1. Dilution of

the solution simply reduces the number density of the screening counterions and aggregates in solution, thereby increasing both the surface potential and the Debye length.

In contrast, the weaker force and an adhesive force minimum of  $-1.5$  mN/m measured in the directly injected 0.05 wt % solution (see Figure 3) point out that the bilayer composition is different from that when adsorption occurs at a higher surfactant concentration. Since the contribution of van der Waals attraction at a separation of 90 Å is small ( $F/R = 0.0015$  mN/m), there is an additional attraction between the bilayers adsorbed at lower concentration. A lower packing density of the bilayer adsorbed from solutions at lower surfactant concentration would leave the hydrocarbon chains of some of the surfactant molecules exposed to the aqueous environment. This is likely due to insufficient time for equilibration. An additional long-range attractive force ("hydrophobic attraction") has been previously measured between such lower density or "depleted" bilayers.<sup>2</sup> A similar screening length in the two cases indicates that the ion and aggregate concentrations in the two solutions are similar.

Addition of 0.01 and 0.10 M salt to 0.05 wt % vesicle solutions not only decreases the range of repulsion but also changes both the surface charge density and the surface potential (Figure 5). The surface charge density  $\sigma_o$  of the bilayers increases from 7.0 mC/m<sup>2</sup> in a solution with no NaCl to 28 mC/m<sup>2</sup> at 0.10 M salt. With the addition of NaCl, the tosylate counterions, which are relatively more hydrophobic and likely bound into the bilayer, are replaced from the vicinity of the CTA<sup>+</sup>-rich bilayers by the relatively more hydrated chloride ion resulting in a net higher surface charge density.<sup>50,53,54</sup> Over the same change in NaCl concentration there is also a significant drop in  $\psi_o$  from 76 to 36 mV.

However, at 0.5 M additional salt, the long-range electrostatic repulsion between the bilayers is sufficiently screened that the vesicles in solution adhere to the mica surfaces and to each other, most likely forming a multilamellar phase. A freeze-fracture electron micrograph of this solution (Figure 6) shows large multilamellar structures formed by aggregation and fusion of these vesicles. This is consistent with an increase in turbidity of the bulk solution, suggesting the growth of larger particles and aggregation of vesicles. In the force measurements, multilayer adsorption onto the mica surfaces gives rise to a long-range repulsion starting at about 100 nm (Figures 5 and 6). The two jumps-in observed in the forces are likely due to the expulsion of one or more bilayers upon compression. A more detailed phase diagram, with an additional electrolyte as a fourth component, needs to be generated in order to completely understand the salt-induced structural changes that occur in spontaneous vesicle-forming systems. This is especially important to explain the stability of the single-phase lamellar region that extends up to roughly 80 wt % surfactant on both the cationic- and anionic-rich sides of the ternary phase diagram. Electrostatic interactions would necessarily only play a minor role at these high surfactant concentrations due to the screening effects of the counterions. Quite often, enhanced undulation repulsions due to very flexible bilayers are necessary to allow for such high water content lamellar phases.<sup>22,41,42</sup> Such undulations cannot be measured with the SFA.

In pure CTAT solution at 0.05 wt % (Figure 7) an oscillatory force profile with a period of about 3 nm is superimposed on a background of electrostatic repulsive force. An oscillatory force with a period of about 10 nm was measured previously in pure cetyltrimethylammonium bromide (CTAB) solutions.<sup>39,40</sup> These oscillatory

forces between bilayers adsorbed on mica from CTAB solutions containing spherical micelles were ascribed to a combination of structural and depletion forces as the micelles were first overpacked and then excluded from the region between the mica sheets as the separation was decreased.<sup>39,40</sup> The oscillation minima are determined by the osmotic pressure induced by excluding the micelles from the solution between the mica surfaces. However, the oscillations shown for pure CTAT are more than an order of magnitude greater in amplitude than the ones seen in CTAB solutions, the oscillation periods are much shorter, about 3 nm as opposed to 10 nm or more, and the oscillations are superimposed on relatively large repulsive electrostatic forces.<sup>39</sup> A second possibility is that the micelles present in pure CTAT solutions under these conditions are rod-like rather than spherical. Similar oscillatory forces have been observed in films of molten polymers;<sup>55</sup> the period of the oscillations is close to the diameter of the polymer chain, and the magnitude of the oscillations is similar to that for the pure CTAT system. Although literature reports<sup>54</sup> suggest that the sphere to rod transition for CTAT micelles occurs at about 10 mM or 0.5 wt % CTAT, the surface force measurements are more consistent with those in polymer systems, suggesting that rod-like micelles are present. At room temperature, both 0.05 and 0.1 wt % CTAT solutions exhibit distinct non-Newtonian flow behavior, also indicative of rod-like micelles being present at these concentrations. From Figure 7, the period of the oscillation in the CTAT solutions is about 3 nm, which is in good agreement with the expected diameter of both spherical and cylindrical micelles. Addition of the negatively charged SDBS to the CTAT solution converts the force profile (Figure 7) to a purely repulsive one, similar to those shown in Figure 2.

In addition to the long-range electrostatic repulsion and the additional short-range repulsion, surface force measurements between catanionic bilayers reveal distinctly different adhesion and fusion characteristics as compared to typical bilayer-forming surfactants. The applied pressure to initiate fusion, calculated from the force and flattened contact area at fusion, for the catanionic bilayers was  $6 \times 10^4$  Pa or about 0.6 atm. In pure lipids and in single-tailed surfactant solutions, in the absence of impurities or fusogenic agents such as hexane, calcium, or fusion proteins, bilayers supported on mica do not fuse, even when under pressures exceeding 40 atm.<sup>2</sup> Although the net interactions were monotonically repulsive in our catanionic bilayers, fusion could be induced at applied pressures orders of magnitude lower than for phospholipid or single-component surfactant bilayers.<sup>2</sup> As bilayer fusion requires nucleation and growth of one or more defects in the bilayer, this reduced pressure for fusion suggests that the nucleation of such defects is much more facile in catanionic bilayers than in phospholipid bilayers. This is likely due to the bilayer edge-stabilizing effect of the excess single-tailed surfactant.<sup>35</sup> In fact, we have observed stable bilayer edges at the surfaces of multilamellar aggregates in the coexistence regime of the phase diagram (see Figure 9B).

However, fusion can be induced at lower pressures by depleting single-component surfactant or phospholipid bilayers by lowering the bulk concentration of surfactant to less than the cmc, which renders the bilayers more hydrophobic and hence induces an attractive hydrophobic interaction.<sup>2</sup> A large hydrophobic force is invariably measured in systems in which fusion occurs spontaneously, for example, in fusion measurements of highly depleted CTAB bilayers.<sup>2</sup> Typically, when fusion occurs

(53) Chen, Y. L.; Chen, S.; Frank, C.; Israelachvili, J. N. *J. Colloid Interface Sci.* **1992**, *153*, 244.

(54) Gamboa, C.; Sepulveda, L. *J. Colloid Interface Sci.* **1986**, *113*, 566. Gamboa, C.; Rios, H.; Sepulveda, L. *J. Phys. Chem.* **1989**, *93*, 5540.

(55) Horn, R. G.; Israelachvili, J. N. *Macromolecules* **1988**, *21*, 2836.

easily, the bilayers jump into an adhesive well at monolayer contact (one bilayer between the mica surfaces). However, for our systems, the concentration range is well in excess of both the critical aggregation concentration of the mixed surfactant and the critical micelle concentrations of both pure surfactants. In addition, only a negligible adhesion energy was observed after separating the fused catanionic bilayers, consistent with the purely repulsive interactions measured in this system. For more typical single-component bilayers, this adhesion energy ranges from 5 to 15 mN/m depending on the extent of bilayer depletion.<sup>2</sup>

In all previous studies, two surfactant bilayers always fused to form a bilayer leaving a monolayer of surfactant on each surface. This phenomenon is referred to as "hemifusion" or "monolayer" fusion. Phospholipid bilayers also show similar hemifusion behavior. Unlike pure surfactant bilayers, fusion of spontaneous vesicle bilayers could be induced by applying pressure in the absence of fusogenic agents and without depleting the bilayers. Bilayer fusion occurred even in the absence of the long-range hydrophobic attraction that was always measured when pure surfactant bilayers were observed to fuse. Another important difference was that fusion in mixed bilayers led from two bilayers between the mica surfaces before fusion to a monolayer of surfactant after fusion. A final surface separation of 1.9 nm between the two bilayers fused is due to "interdigitation" of the two monolayers. The final thickness measured is only marginally greater than the thickness of a monomolecular layer measured in other experiments in this study. This novel fusion behavior is also a factor in the unusual stability of vesicles in solution even at significantly high vesicle volume fractions.

### Conclusions

Detailed surface force measurements between bilayers adsorbed onto mica surfaces from solutions containing

equilibrium vesicles of the single-tailed cationic surfactant CTAT and the anionic surfactant SDBS show significant differences from the interactions of typical bilayer-forming phospholipids. The most important to the stability of the catanionic vesicles is the absence of an adhesive minima due to the large electrostatic double-layer interactions between the charged bilayer surfaces. The magnitude of the double-layer forces makes the bilayer interaction repulsive at all separations and is significantly larger than any repulsion due to bilayer undulations. This shows that catanionic vesicles are *unconditionally* stable against aggregation at dilute concentrations. However, at high ionic strength (which occurs in the presence of added electrolyte, at the surfactant concentrations present near the transition from the vesicle to the lamellar phase, and in the lamellar phase), screening diminishes the electrostatic interactions to the point that requires a different, and as yet, unknown mechanism of bilayer repulsion. In addition, as the phase diagram shows (Figure 1a), vesicle phases occur up to a nearly 1:1 cation to anion ratio, where the bilayers would be nearly neutral and electrostatics should play only a minor role. Hence, it appears as if there may be other possible explanations for catanionic vesicle stability over different composition ranges that require further investigation.

**Acknowledgment.** We thank T. Kuhl and S. Steinberg for helpful discussions. J.A.Z., S.C., J.I., Z.X., and E.N. acknowledge partial support by the NIH under Grant GM47334 and by the NSF under Grant CTS-9212790. J.A.Z., E.K., and K.H. were supported by the NSF under Grant CTS-9319447. We acknowledge use of the facilities provided by the Materials Research Laboratory supported by the NSF under Grant DMR-9123048.

LA950233H